

3D Bioprinting Pancreatic Cancer Cells

Technical Report
Presented to the Faculty of the
School of Engineering and Applied Science
University of Virginia

By

Suzanne Lightsey

May 1, 2020

3D Bioprinting Pancreatic Cancer Cells

Authors: Suzanne Lightsey, Shayn Peirce, Christopher Highley, Matthew Lazzara

Abstract

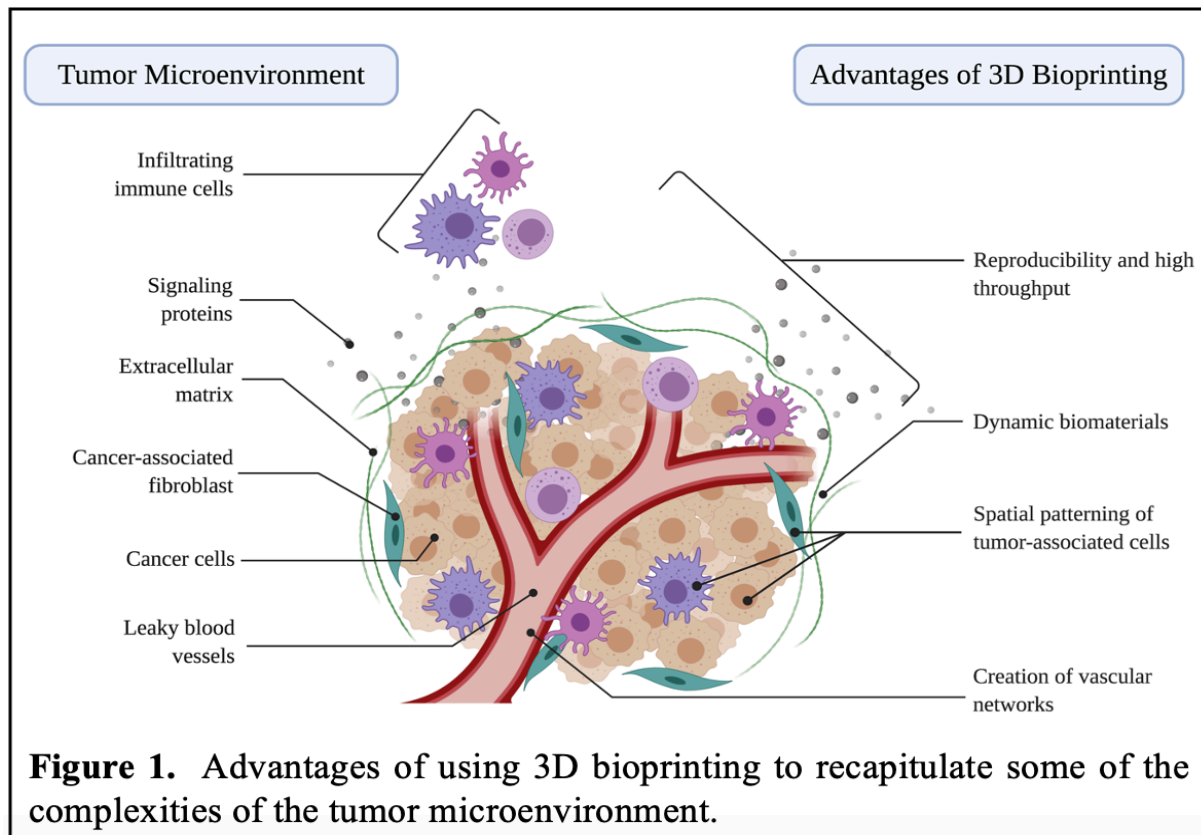
In this review paper, design decisions associated with 3D bioprinting are described and future opportunities to enhance the use of 3D bioprinting in cancer research are presented. Conventional *in vitro* models used to study cancer, both two-dimensional and three-dimensional, cannot mimic all of the complexities of the tumor microenvironment in cancer. Through the creation of more physiologically relevant *in vitro* models, a deeper understanding of the mechanisms that facilitate tumor progression will allow for better cancer therapy. 3D bioprinting serves as a promising alternative to traditional methods of model fabrication because it offers the ability to create complex architectures with tumor-associated cells using dynamic biomaterials. The state of the art in specific topics reviewed in this study are: biomaterials, cell types, 3D bioprinting parameters, and methods of analysis. An illustrative case study based on the author's research is presented.

Introduction

Cancer is the second-leading cause of death in the United States with a projected 1,806,590 new cancer cases and 606,520 cancer-related deaths in 2020 [1]. Despite significant efforts by researchers, drug development for cancer has remained slow in the past decade, with over 95% of drugs failing during clinical trials [2]. Two main factors have been attributed to this high failure rate: (1) the inherent complexity of cancer as a disease and (2) the oversimplification of preclinical models. There are hundreds of types of cancer, with complex genetic variations within a single cancer type, making the development of a generic cure for cancer both difficult and expensive [3,4]. Due to the intricate nature of this disease, preclinical models used to recapitulate tumors in

patients are grossly oversimplified, making them a poor representation of the compounded interactions between the tumor and its environment [5,6].

Indeed, new research has shown that the use of three-dimensional (3D) cancer models over the traditional two-dimensional (2D) models can lead to significantly different gene and protein expressions, cell morphologies, cell-cell and cell-matrix interactions, and differentiation [7-9]. The differences between these models is correlated with the evolving notion that tumors, which used to be considered as merely a mass of proliferating cancer cells, are comprised of a 3D network of stromal, immune, and endothelial cells nested in a dynamic extracellular matrix (ECM) that supports and mediates tumor therapeutic sensitivity and resistance as shown in Figure 1 [10]. Various technologies have been developed to model specific aspects of the complex tumor microenvironment *in vitro* ranging from simplistic spheroids models to more advanced, engineered organoids. These technologies aim to increase the spatiotemporal control in a more physiologically



relevant context; however, major challenges associated with current 3D *in vitro* models include their limited vasculature potential, lack of tissue-tissue interfaces, such as interactions between surrounding connective tissue, and these models are generally devoid of exposure to mechanical cues [11,12]. As a result, most current models concentrate on reproducing specific, basic functions of the respective tissue instead of macroscopic interactions across interfaces.

3D bioprinting offers an appealing approach to overcome many of the aforementioned limitations due to its ability to create complex architectures in an efficient and reproducible manner. While there are already many excellent review papers detailing different bioprinting methods, their limitations, and their biomedical applications, here we enumerate the design decisions associated with using 3D bioprinting to generate model systems for cancer research [6, 10, 11, 12, 15, 16, 24, 27, 30]. In addition, we describe how 3D bioprinting technology can overcome the limitations of existing model systems to advance cancer research, present a case study on how 3D bioprinting is used to create a model system, and suggest opportunities for future studies to enhance the use of 3D bioprinting in cancer research.

Current approaches using 3D bioprinting for generating *in vitro* cancer models

Bioprinting is defined as the spatial arrangement of living cells, biological materials, and biochemicals using a computer-aided layer-by-layer deposition process in order to fabricate 3D structures for regenerative medicine, pharmacokinetic, and biological studies [13]. There are three main technologies used for deposition and patterning of biological materials: inkjet, stereolithography, and extrusion bioprinting. Inkjet and stereolithography bioprinters both offer unique properties; however, they are limited in that they cannot print high cell densities due to needle clogging and light scattering, respectively [14,15]. Extrusion bioprinting involves extruding

a bioink through a nozzle using either a pneumatic or piston-controlled computer system. The bioink is continuously deposited layer-by-layer to form a 3D structure. In order for the 3D structure to maintain its integrity, a bioink with a high viscosity is necessary until the material is crosslinked using either physical, enzymatic, or chemical methods [16]. Extrusion bioprinting offers a simple and cost-effective process; however, cell viability can be affected due to the shear stress that is induced during the extrusion process.

Despite these limitations, extrusion bioprinting is currently the most commonly used bioprinting technique in cancer research and, as a result, will be the method exclusively discussed throughout this review. The main reasons for its success as a model system in cancer research are its simplicity, its low investment cost, and the capability to print both viscous bioinks and a high density of cancer cells [15]. Extrusion printing's freeform nature allows users to implement innovative modifications to their system thus allowing unique experimental designs.

A study conducted by Xu et al. pioneered the use of extrusion-based bioprinting in 2010 [17]. In this study, ovarian cancer cells and normal fibroblasts were spatially patterned onto a Matrigel substrate. Extrusion printing allowed the researchers to precisely control the cell positioning and, as a result, increase the reproducibility of the models. Xu et al. showed that the bioprinted model was comparable to cells originally ejected by manual pipetting and could serve as a physiologically relevant ovarian cancer coculture model to gain a better understanding of ovarian cancer biology. Following this study, researchers set out to use extrusion bioprinting to study cancer biological questions that were previously not feasible. A study by Lee et al. examined the cell-cell interactions between vascular cells and glioblastoma (GBM) cells by placing patient-derived GBM cell clusters close to bioprinted fluidic vessels [18]. Similarly, Grolman et al. used bioprinting to surround a channel of macrophages with breast adenocarcinoma cells to model an

example of a paracrine loop that regulates metastasis [19]. Extrusion bioprinting was essential in the study conducted by Grolman et al. because it is the only bioprinting technique that allows for the fabrication of a core-shell construct, a shape that appears often physiologically.

The aforementioned studies used extrusion bioprinting to provide a more relevant tumor microenvironment to better understand cell-cell interactions and tumor-progression mechanisms. However, 3D bioprinting can also be used to investigate more clinically relevant questions. For example, Zhao et al. and Dai et al. bioprinted a cervical and a glioma tumor model, respectively, and found that the 3D printed tumor model was more resistant to therapy when compared to 2D culturing [20,21]. Two additional studies moved the bioprinting field forward by using extrusion-based printing to reconstruct the tumor microenvironment. Langer et al. utilized the core-shell technology to surround cancer cells with endothelial cells and fibroblasts [22]. They were able to create a scaffold-free 3D model to study tumor-stromal interactions and allow for the cells within the bioprinted tissues to mature, self-organize, and deposit matrix proteins. A study by Meng et al. used bioprinting techniques to build tumor constructs via precise placement of living cells, consisting of lung cancer cells, fibroblasts, and endothelial cells, functional biomaterials, and programmable release capsules [23]. This unique approach provided the researchers with the spatiotemporal control of signaling molecular gradients and, as a result, control over cellular behaviors at a local level. Each of these published studies made numerous design decisions about the biomaterials used, types of cells, cell densities, and methods of analysis. These design considerations and their implications are described in more detail below.

Biomaterials

For bioprinting to be successful, dynamic biomaterials that can support the cellular components during and after fabrication must be integrated into the system. Biomaterials are

separated into two classes: synthetic and natural. Natural biomaterials, such as collagen, hyaluronic acid, or alginate, have excellent biocompatibility and intrinsic cell-adhesion ligands; however, their weak mechanical properties and difficult manipulation can be a challenge during bioprinting [24]. On the other hand, synthetic biomaterials, such as PEG or PCL, can have their chemical and physical properties easily tuned to adjust parameters like mechanical stiffness, degradation rate, and bioactivity [12, 25, 26]. Typically, natural biomaterials are often combined when used for extrusion printing due to the systems reliance on material properties for printing. Materials used for extrusion printing must be nearly fluid to flow through the small diameter nozzle, but they must also mechanically strong enough to support themselves after deposition. Common biomaterials used for bioprinting tumor models include gelatin, alginate, fibrin, methacrylated gelatin (GelMA), and sacrificial materials [18-23].

Gelatin

Gelatin is derived from collagen that has undergone partial hydrolysis. The melt temperature of this degraded product typically lies between 30 and 35°C, thus limiting gelatin's application to experiments that are below physiological temperatures [27]. Despite this limitation, gelatin is naturally cell-adherent and its temperature-sensitivity allows for easy extrusion [28]. Often, gelatin can be used as a thickener to make other biomaterials more viscous for extrusion bioprinting.

Alginate

Alginate is a polysaccharide found within the cell walls of brown algae. Alginate has been extensively researched for regenerative medicine due to its ability to form a hydrogel through an almost instantaneous sodium-calcium ion exchange reaction. Due to alginate's fast gelation time, it is commonly used to create hydrogel capsules containing pancreatic islets [29]. While alginate

is a promising bioink, its rapid gelation time can make it difficult to control the geometry and, as a result, it is not often printed alone, but rather combined with other natural materials [27].

Fibrin

Fibrin is a naturally occurring protein that helps with blood clotting and wound healing in the body. As a result, this biomaterial has excellent biocompatibility and biodegradation properties, but weak mechanical properties. Similar to alginate, fibrin hydrogels have a rapid gelation time through crosslinking fibrinogen with an enzymatic treatment of thrombin [30]. This fast gelation time can also make it difficult to control the geometry of the bioprinted construct, and thus is often mixed with other natural materials.

Methacrylated gelatin (GelMA)

GelMA is a synthetic biomaterial that consists of gelatin with methacryloyl side groups which, when exposed to UV light, can become covalently crosslinked with the presence of a photoinitiator. GelMA has also been shown to maintain high cell viability at lower concentrations (≤ 5 w/v%) [31]. However, at lower concentrations GelMA has a low viscosity, causing instability during the extrusion process, resulting in irregular filament shapes [32]. It is possible to increase the bioink's viscosity by increasing the concentration of GelMA, but there is a trade-off between the viscosity and the cell viability.

Sacrificial bioinks

Not all biomaterials used during the bioprinting process must remain in the final cancer model system. In fact, synthetic materials have been designed to act as placeholders during the printing process, but then be washed out, leaving voids in the final model. This technique is often used to create bioprinted vasculature through bioprinting a permanent gel and a sacrificial gel sequentially on top of each other [11]. The permanent gel is then crosslinked and, afterwards, the

sacrificial gel is removed through either a chemical or physical process. This leaves behind channels that can be perfused with endothelial cells, thereby resulting in the vascularization of a complex bioprinted model system.

Cell types

In order for tumors to progress from the normal to the malignant state, heterotypic interactions between the cancer cells and multiple distinct non-malignant cell types are necessary in the tumor microenvironment. It has been shown that for a number of cancers, including colorectal cancer, pancreatic cancer, and prostate cancer, that an increased portion of stroma relative to tumor mass is associated with a decrease in patient survival [10]. Indeed, cancer cells can orchestrate changes to their environment through recruiting cancer-associated fibroblast, infiltrating immune cells, and establishing tumor vasculature networks [33]. Together, these changes to the tumor's microenvironment can modulate its sensitivity to therapy and treatment. As a result, tumor models containing only cancer cells have little physiological relevance for clinical applications. In this next section, the cell components of the tumor microenvironment are briefly outlined and the advantages in recapitulating these components in model 3D-bioprinted tumor systems are described.

Cancer-associated fibroblasts

Cancer-associated fibroblasts (CAFs) are abundant in the tumor stroma of many epithelial cancers and have been shown to encourage cell survival, angiogenesis, and invasion [34]. CAFs deposit ECM components and produce enzymes that dramatically remodel the tumor's matrix. This remodeling frequently displays aligned collagen fibers that can serve as highways on which tumor cells are observed to migrate on *in vivo* [35]. CAFs have also been shown to contribute to therapeutic resistance through ligand-dependent activation of receptor tyrosine kinases, thus

indicating that co-targeting tumor cells and CAFs may be an effective way to improve therapeutic treatment [34]. The aforementioned studies by Xu et al., Langer et al., and Meng et al. included fibroblasts in their model system to increase the overall biological relevance of their *in vitro* model [17, 22, 23].

Immune cells

Over the last decade, it has been predicted that both the innate and the adaptive immune systems can have a paradoxical impact on tumor progression, both being able to promote and prevent the disease. There are currently three processes that describe cancer immunology: elimination, equilibrium, and escape [10]. Initially, tumor growth incites an inflammatory response that recruits innate immune cells to the site. Next, the immune system is able to contain the tumor growth, but not fully eradicate the cancer cells, thus entering the equilibrium process. During this time, the surviving cancer populations can mutate to gain resistance to immune detection and finally escape into the surrounding environment.

Advancing our understanding of how immune cells modulate the tumor microenvironment and disease progression can help researchers target novel anti-cancer strategies that could either increase adaptive immunity or neutralize some of the cancer-promoting properties of innate immune cells [33]. The study conducted by Grolman et al. showed that interactions between breast cancer cells and macrophages primes the tumor cells for intravasating into the bloodstream [19]. Through the ability to 3D bioprint immune cells with cancer cells and fibroblasts, scientists can gain a better understanding of the mechanisms behind these processes, thus improving the survival for many cancer patients.

Vascular endothelial cells

During tumor progression, cancer cells recruit blood vessels and induce the formation of abnormal vessels through angiogenesis. These vessels are often leaky and poorly organized, increasing the interstitial pressure within the tumor and impairing the blood flow to cancer cells. As a result, a hypoxic and necrotic environment is facilitated, which has been shown to make tumors more aggressive [10]. The poor perfusion also makes drug delivery to the target cells more challenging.

Due to the complex nature of this system, researchers have heavily relied on potentially costly animal models for *in vitro* studies [36]. However, bioprinting has the unique ability to use sacrificial inks to create organized vessel-like structures in 3D systems. Utilizing the spatial control that bioprinting affords, researchers can now generate 3D models with leaky vessels to better study the recruitment of blood vessels to tumors, cancer cell migration across blood vessels, and the impact of more relevant fluid forces on cancer-endothelial cell interactions. Interestingly, studies like Langer et al. included endothelial cells as a structural component in their system to provide mechanical stability to their scaffold-free bioprinted tissue, rather than to study vasculature and angiogenesis in tumor models [22]. More research is needed to conclude if endothelial cells could be used to increase bioprinted tissues's stability.

3D Bioprinting Parameters

A few important parameters to consider before selecting a 3D bioprinted model system that have not been previously discussed are: cell density, shape and size of constructs, and patterning within the printed constructs. For recreating the tumor microenvironment, extrusion bioprinting allows for the initial printed cell density to closely mimic the high cell density seen in tumors. Also, a more relevant distribution of cell densities can be achieved by using multiple nozzles during bioprinting [16]. When selecting the constructs' shape, it is important to ensure the size of

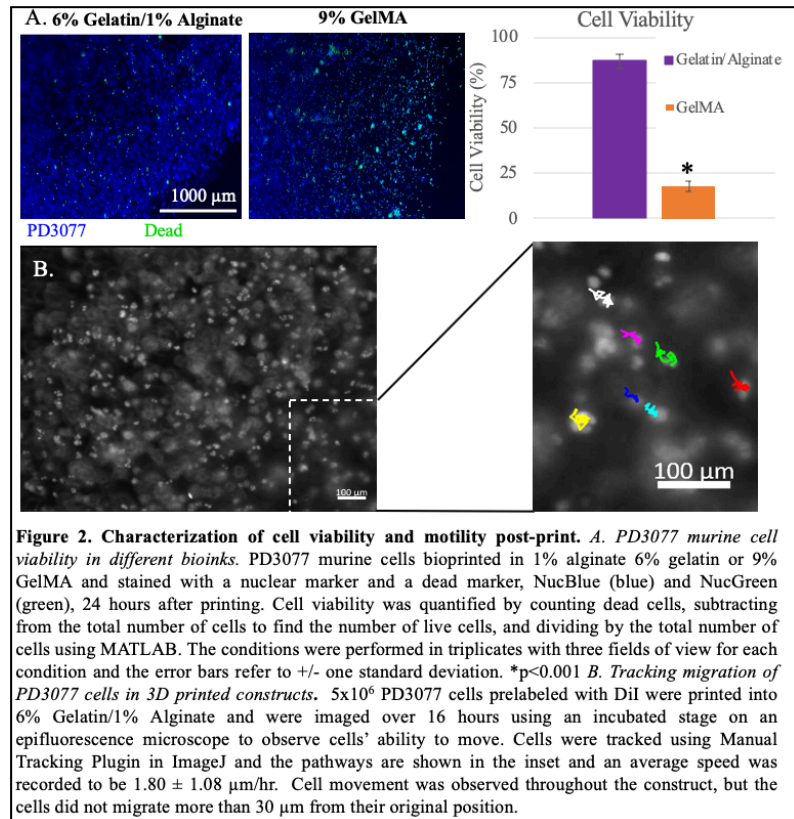
the construct allows for sufficient diffusion of nutrients to the cells in order to prevent a necrotic core from forming. It is also critical to strategically select the construct's shape to address the application. For example, if a researcher wants to study cell-cell interactions between the stroma and tumor, a core-shell shape would be sufficient. However, if the researcher prefers to ask a question on the effect of fluid forces on drug delivery, using a sacrificial ink to form channels would be more appropriate. Finally, for extrusion bioprinting when ink is deposited, there is a slight displacement of previously-laid biomaterial. Therefore, if a solid shape is desired the use of concentric circles is preferable over a checkered pattern.

Methods of Analysis

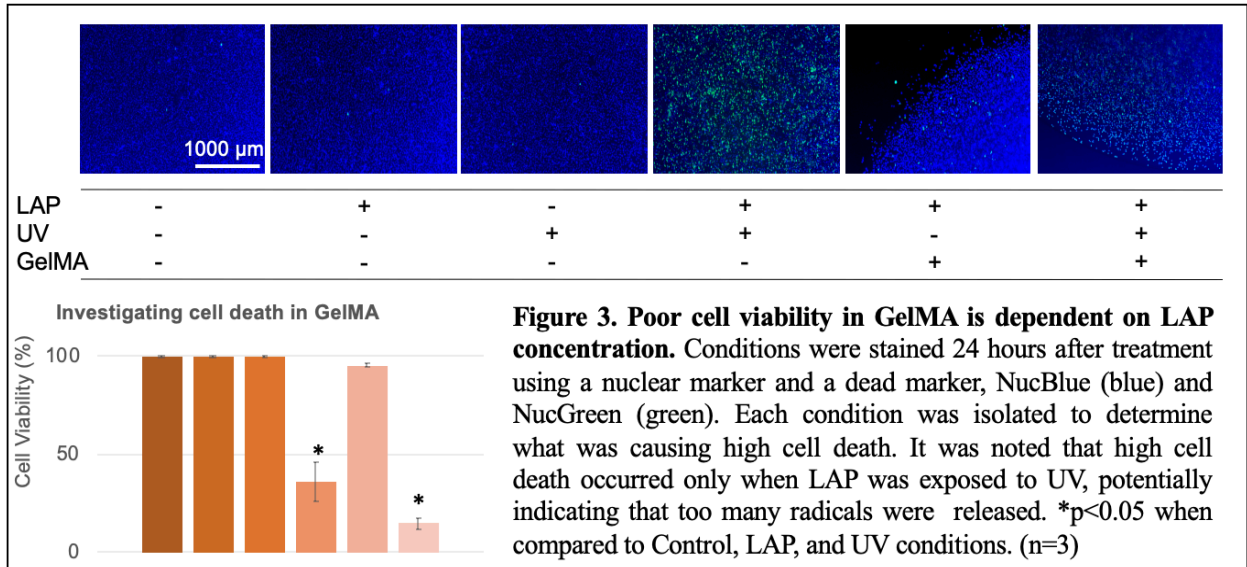
Because 3D bioprinting offers many opportunities to customize a system, there has been little development towards creating standard methods of analysis for these printed constructs. Parameters like cell viability, migration speed, imaging through 3D spaces, checking for a necrotic core, etc., have been measured using copious techniques. As a result, translating studies across researchers can be a significant challenge, and this has contributed to the slow progress in bioprinting development [37]. Today, there is a serious need to create a more robust bioprinted system that can be replicated easily and used widely for *in vitro* cancer studies.

Case Study

The first step in developing a 3D bioprinted system was to identify a viable bioink. Here, we developed new protocols to investigate two bioinks for their ability to recapitulate some of the biochemical and biomechanical complexities of the tumor microenvironment: (1) an alginate-derived hydrogel comprised of 1% alginic acid

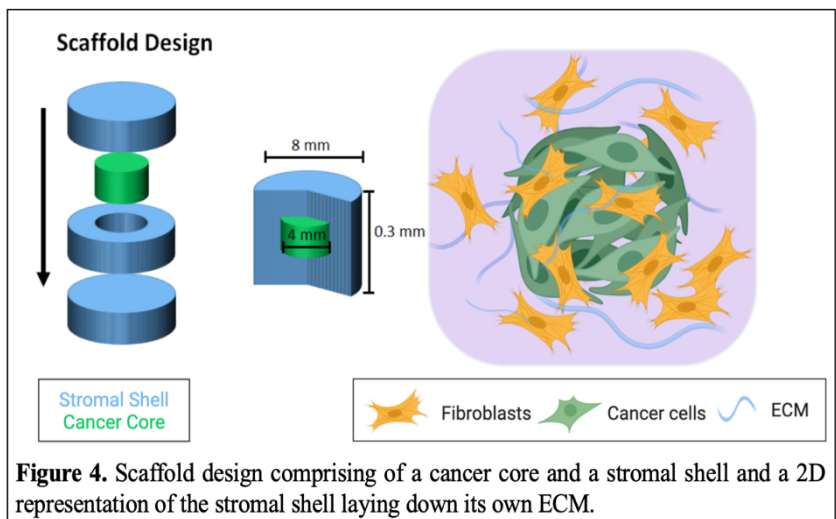


sodium salt powder and 6% gelatin and (2) a 9% w/v methacrylated gelatin (GelMA) [38, 39]. Due to the thermosensitivity of gelatin, temperatures ranging from 23°C to 30°C were investigated; 28°C was identified as the ideal printing temperature to produce gels with appropriate mechanical properties. Live/dead assays showed an 87% cell viability in the alginate-derived bioink for murine pancreatic ductal adenocarcinoma (PDAC) cells in culture 24 hours after printing whereas a 18% cell viability was observed in GelMA constructs, indicating that GelMA may not be an ideal bioink for future PDAC studies (Fig. 2A). Cell motility was also observed in the alginate-derived constructs through time-lapse imaging four days after printing. However, the cell movements observed did not display strong directional migration, as typically observed for the same cell line on tissue culture plastic (Fig. 2B). These results provide a reproducible method to print cancer



cells in an alginate-derived hydrogel while maintaining high cell viability as well as some degree of cell motility. Interestingly, after investigating the cause of the low cell viability in GelMA, the author was able to identify that cell death occurred when the photocrosslinker, lithium phenyl-2,4,6-trimethylbenzoylphospinate (LAP), was exposed to UV (Fig. 3). The UV light used a wavelength of 365 nm for which LAP has a significant absorbance [40]. Due to this, we hypothesized that too many radicals may be generated while the constructs are being crosslinked.

Because of the limited cell motility observed in the alginate-derived bioink, we proposed a 3D bioprinting approach similar to Langer et al. in which a cancer core is surrounded by a stromal shell as shown in Figure 4 to create a scaffold-free bioprinted tissue [22]. This method can be achieved by utilizing the alginate-derived bioink previously established and printing at very high cell



densities of 1.5×10^8 cells/mL of bionk to gain the necessary mechanical properties for printing. The cell paste allows the bioprinted tissue to self-organize and deposit matrix proteins rapidly, so that an enzyme treatment can be used at 48 hours to remove the biomaterials used, leaving a purely cellular structure behind. This approach is promising because it allows the opportunity to bypass the motility limitations observed in the bioink.

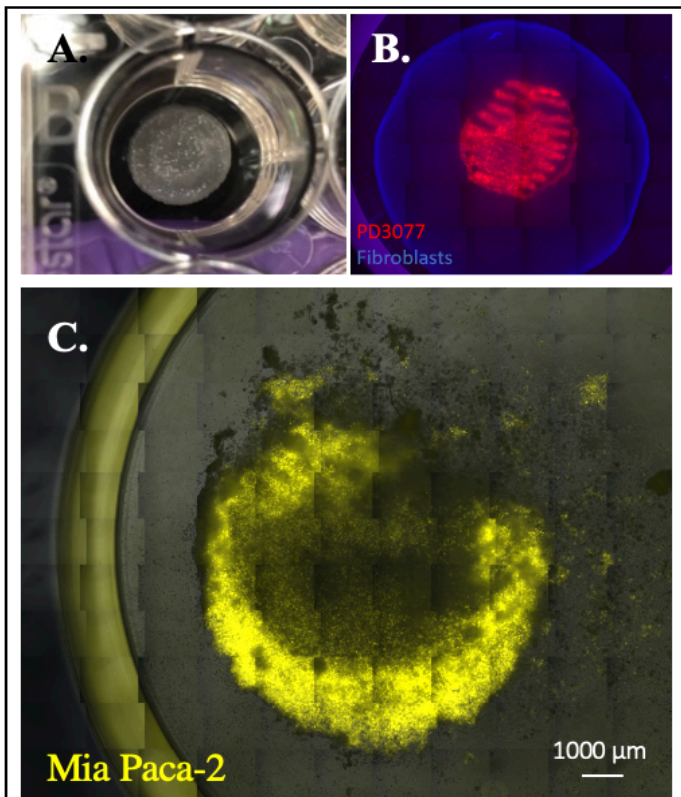


Figure 5. 3D bioprinted core-shell design. *A.* A photograph of a bioprinted construct before being crosslinked. *B.* Epifluorescent, tiled image of PD3077 cells, labeled with DiI, printed in a core shape surrounded by fibroblasts labeled with NucBlue. *C.* Epifluorescent, tiled image of BFP+ MIA PaCa-2 cells printed in a core shape surrounded by unlabeled fibroblasts 24 hours after treatment with Alginate Lyase.

A photograph of the core-shell construct before being crosslinked is shown in Figure 5A and a fluorescent image showing the precise positioning of the cell sub-types is seen in Figure 5B. Unfortunately, after these constructs underwent the enzyme treatment, they lost their mechanical stability and fell apart upon further culturing (Fig. 5C). Despite this setback, preliminary results showed that constructs undergoing treatment relaxed, thus restoring cell movement.

Future work involves incorporating endothelial cells into this system, to determine whether intact networks of endothelial cells will form across the

construct and provide mechanical stability to the bioprinted tissues. Once the 3D bioprinted tissue is rendered stable after the enzyme treatment, follow up studies could be conducted investigating

the system's migratory response to varying the ratio of epithelial and mesenchymal pancreatic tumor cells. Through this analysis, we could identify which phenotypic make-up has more oncogenic properties and therefore is more likely to enable tumor cell invasion and intravasation *in vivo*.

Discussion

In this review, many of the design decisions available for 3D bioprinting model systems for cancer research are described. Although bioprinting is used for many tissue-engineered therapies, its ability to precisely engineer tissue composition, spatially pattern cells, and create vasculature at a high throughput make it particularly appealing for cancer research. Specifically, the case study presented explored different biomaterials, designs, and cells needed to create a reproducible method to pattern cancer cell sub-types while maintaining high cell viability and some degree of motility. In particular, it is important to note that GelMA, a well-established bioink, was not suitable for bioprinting pancreatic cancer cells, despite it being shown to effectively support other cancer cells, thus highlighting the need to design models for different cancer types [32]. Despite the advances this case study made in modeling the pancreatic tumor microenvironment, both vasculature and mechanical stability are needed for this model to be physiologically relevant.

It is also important to note that this review primarily focused on extrusion bioprinting due to its design simplicity, low cost, and capability of printing a high density of cells, thus making it appealing for recapitulating the dense tumor microenvironment. However, other methods like stereolithography and ink-jet printing offer unique properties such as high dimensional accuracy and throughput which can also be used to enhance the accuracy of 3D bioprinted cancer models.

Although bioprinting technologies over the last decade have rapidly evolved, further development of biomaterials designed specifically for bioprinting is needed. Current biomaterials used for cancer models are comprised of one or more extracellular proteins to support cellular functions after being bioprinted. However, due to the complexity of the native extracellular matrix structure, these materials do not accurately mimic the tumor microenvironment. The scaffold-free bioprinted tissue is a promising candidate because it allows tumor-associated cells to self-organize and deposit matrix proteins more indicative of what would be seen *in vivo*. Decellularized extracellular matrix is another novel material that could be used as a feasible bioink precursor [41]. This biomaterial could be derived from the patient's own tissues and offers inductive cues to support cell growth.

3D bioprinting offers the potential to create *in vitro* tumor models that are more physiologically relevant and thus clinically translational. Through the creation of better *in vitro* models, it would be possible to better test drug therapies and predict the most effective drug type and dosage from specific cancer types. However, further development of a robust protocol is needed to quantify bioprinted systems that can encompass cancer types before this future is feasible. Additional studies in these highlighted areas will foster more collaboration between researchers, thus covering a wider range of cancer types and significantly improve cancer drug efficacy rates.

Materials and Methods

Cell culture

All cell lines were grown in standard tissue culture conditions at 37°C with 5% CO₂. Murine PDAC cells (PD3077), human pancreatic carcinoma cells (HPAFII and MIA PaCa-2), and

human pancreatic CAFs (0082T) were cultured in DMEM supplemented with 10% FBS, 1% 100X GlutaMAX, and 0.2% gentamicin. Before bioprinting, cells were cultured in 15 cm plates to achieve the desired high cell density. Cell lines were maintained at a relatively low passage number for anticipated responsiveness.

Hydrogel precursor synthesis

To form the alginate-derived precursor, 1% w/v of alginic acid sodium salt and 6% of type A porcine skin gelatin were dissolved in DPBS under constant agitation with 600 rpm at 60°C for 1 hour. The solution was sterile filtered using a 0.45 µm filter and stored at 4°C. In order to prepare the GelMA precursor, 10% w/v of type A porcine skin gelatin was dissolved in PBS at 60°C. Methacrylic anhydride was then added to the gelatin solution at 50°C at a rate of 0.5 ml/min to generate a 20% (v/v) solution of GelMA within a chemical fume hood. After 3 hours, a 5-fold dilution was performed with the addition of warm PBS and the solution was dialyzed for seven days. The solution was then frozen, lyophilized, and stored at -20°C until further use.

3D bioprinting of single-layer disk

PD3077 murine cells were suspended in the both the alginate-derived hydrogel and GelMA at 37°C with a density of 5×10^6 cells/mL and printed using a RegenHU 3DDiscovery bioprinter. For optimal printing viscosity, the alginate-derived hydrogel was heated to 28°C before printing. To generate tissues, the bioink mixes were loaded into CELLINK UV shielding cartridges fitted with a 27G needle, listed in Figure 6, and extruded directly onto a 24-well plate using pressure ranging from 0-2 bar. The printed constructs consisted of a single-layered disk with a radius of 5 mm and a height of 200 µm. This disk geometry was selected in order to achieve a region of densely packed cells that is capable of representing the *in vivo* tumor cell-cell interactions. The alginate-derived and GelMA constructs were then crosslinked using 2% CaCl₂ for 5 minutes and

UV light for 30 seconds, respectively. Tissues were maintained up to 7 days, with media exchanges every other day.

3D bioprinting of core-shell configuration

3D bioprinted cancer tissues were fabricated using a RegenHU 3DDiscovery bioprinter. The cells for each compartment (stromal or cancer) were combined and resuspended in the alginate-derived hydrogel at 37°C to a final concentration of 1.5×10^8 cells/mL. To generate tissues, the cancer and stromal bioink mixtures were loaded into CELLINK UV shielding cartridges fitted with a 27G needle, the stromal shell was warmed to 28°C using a temperature sleeve, and then both were extruded directly using pressure between 0-2 bars onto a 24-well plate with the design shown in Figure 4. Tissues were treated with a buffered solution containing 2% calcium chloride for 5 minutes in order to crosslink the alginate-containing hydrogel and then were cultured in medium at 37°C. Crosslinked tissues were treated with 0.2 mg/mL of Alginate Lyase 48 hours after printing. In the standard print, the stromal compartment contained CAFS and the cancer compartment consisted of either PD3077, HPAF II, or MIA PaCa-2 cells.

Staining and imaging

To assess cell viability, 3D bioprinted constructs were incubated for 24 hours and labeled to assess cell viability using NucBlue Live reagent and NucGreen Dead reagent from ReadyProbes Cell Viability Imaging Kit at 0.5 drops/mL of medium. HPAF II and MIA PaCa-2 cell lines were transduced with a green fluorescent protein and a blue fluorescent protein, respectively, to visualize the cells temporally. An incubated stage on an epifluorescence microscope was also used to observe cell movement over time. For some prints, PD3077 cells were incubated with membrane stain, DiI, at 0.2 μ L per 1×10^8 cells before printing.

Quantification and statistical analysis

Cell viability was quantified by counting dead cells, subtracting from the total number of cells to find the number of live cells, and dividing by the total number of cells using MATLAB. The conditions were performed in triplicates with three fields of view for each condition. Cell motility in an alginate-derived by prelabeling PD3077 cells with DiI before printing and imaging over 16 hours using an incubated stage on an epifluorescence microscope. Cells were tracked using Manual Tracking Plugin in ImageJ. Statistical significance was determined using either a two-tailed Student's t test or a one-way ANOVA, as denoted in the figure legends. Significance, represented with asterisks, is defined as a p-values less than 0.05.

Item	Vendor	catalog#/ SKU
Gelatin from porcine skin, Type A	Sigma Aldrich	G2500
Alginic acid sodium salt	Sigma Aldrich	180947
Alginate Lyase	Millipore	A1603
Calcium Chloride Dihydrate	Millipore	208290
ReadyProbes™ Cell Viability Imaging Kit Blue/Green	Invitrogen	R37609
UV SHIELDING CARTRIDGES, 3CC, 50 PCS	Cellink	CSO010311502
STERILE STANDARD BLUNT NEEDLES 27G, 50 PCS, 12.7 mm	Cellink	NZ5270505001 (0.50")
DiI cell labeling solution	Invitrogen/Fisher	V22888

Figure 6. Key Resources Table.

References

1. Siegel, Rebecca L., Kimberly D. Miller, and Ahmedin Jemal. "Cancer statistics, 2020." *CA: A Cancer Journal for Clinicians* 70.1 (2020): 7-30.
2. Maeda, Hiroshi, and Mahin Khatami. "Analyses of repeated failures in cancer therapy for solid tumors: poor tumor-selective drug delivery, low therapeutic efficacy and unsustainable costs." *Clinical and translational medicine* vol. 7,1 11. 1 Mar. 2018, doi:10.1186/s40169-018-0185-6.
3. Berger, Michael F., et al. "The genomic complexity of primary human prostate cancer." *Nature* 470.7333 (2011): 214-220.
4. Palanisamy, Nallasivam, et al. "Rearrangements of the RAF kinase pathway in prostate cancer, gastric cancer and melanoma." *Nature medicine* 16.7 (2010): 793.
5. Rubin, Eric H., and D. Gary Gilliland. "Drug development and clinical trials—the path to an approved cancer drug." *Nature reviews Clinical oncology* 9.4 (2012): 215.
6. Wang, Chengyang, et al. "Three-dimensional in vitro cancer models: a short review." *Biofabrication* 6.2 (2014): 022001.
7. Ridky, Todd W., et al. "Invasive three-dimensional organotypic neoplasia from multiple normal human epithelia." *Nature medicine* 16.12 (2010): 1450.
8. Ghosh, Sourabh, et al. "Three-dimensional culture of melanoma cells profoundly affects gene expression profile: A high density oligonucleotide array study." *Journal of cellular physiology* 204.2 (2005): 522-531.
9. Zervantonakis, Ioannis K., et al. "Three-dimensional microfluidic model for tumor cell intravasation and endothelial barrier function." *Proceedings of the National Academy of Sciences* 109.34 (2012): 13515-13520.
10. Fong, Eliza LS, et al. "Heralding a new paradigm in 3D tumor modeling." *Biomaterials* 108 (2016): 197-213.
11. Pati, Falguni, Jesper Gantelius, and Helene Andersson Svahn. "3D bioprinting of tissue/organ models." *Angewandte Chemie International Edition* 55.15 (2016): 4650-4665.
12. Zhang, Yu Shrike, et al. "Bioprinting the cancer microenvironment." *ACS biomaterials science & engineering* 2.10 (2016): 1710-1721.
13. Guillemot, Fabien, Vladimir Mironov, and Makoto Nakamura. "Bioprinting is coming of age: report from the International Conference on Bioprinting and Biofabrication in Bordeaux (3B'09)." *Biofabrication* 2.1 (2010): 010201.
14. Yi, Hee-Gyeong et al. "3D Printing of Organs-On-Chips." *Bioengineering (Basel, Switzerland)* vol. 4,1 10. 25 Jan. 2017, doi:10.3390/bioengineering4010010
15. Oztan, Y. Cagri, et al. "Recent Advances on Utilization of Bioprinting for Tumor Modeling." *Bioprinting* (2020): e00079.
16. Ozbolat, Ibrahim T., and Monika Hospodiuk. "Current advances and future perspectives in extrusion-based bioprinting." *Biomaterials* 76 (2016): 321-343.
17. Xu, Feng, et al. "A three-dimensional in vitro ovarian cancer coculture model using a high-throughput cell patterning platform." *Biotechnology journal* 6.2 (2011): 204-212.
18. Lee, Vivian K., et al. "Generation of 3-D glioblastoma-vascular niche using 3-D bioprinting." *2015 41st Annual Northeast Biomedical Engineering Conference (Nebec)*. IEEE, 2015.

19. Grolman, Joshua M et al. "Rapid 3D Extrusion of Synthetic Tumor Microenvironments." *Advanced materials (Deerfield Beach, Fla.)* vol. 27,37 (2015): 5512-7. doi:10.1002/adma.201501729
20. Zhao, Yu, et al. "Three-dimensional printing of Hela cells for cervical tumor model in vitro." *Biofabrication* 6.3 (2014): 035001.
21. Dai, Xingliang, et al. "3D bioprinted glioma stem cells for brain tumor model and applications of drug susceptibility." *Biofabrication* 8.4 (2016): 045005.
22. Langer, Ellen M., et al. "Modeling tumor phenotypes in vitro with three-dimensional bioprinting." *Cell reports* 26.3 (2019): 608-623.
23. Meng, Fanben, et al. "3D bioprinted in vitro metastatic models via reconstruction of tumor microenvironments." *Advanced Materials* 31.10 (2019): 1806899.
24. Zhang, Yu Shrike, et al. "3D bioprinting for tissue and organ fabrication." *Annals of biomedical engineering* 45.1 (2017): 148-163.
25. Peppas, Nicholas A., et al. "Hydrogels in biology and medicine: from molecular principles to bionanotechnology." *Advanced materials* 18.11 (2006): 1345-1360.
26. Khademhosseini, Ali, and Robert Langer. "Microengineered hydrogels for tissue engineering." *Biomaterials* 28.34 (2007): 5087-5092.
27. Skardal, Aleksander, and Anthony Atala. "Biomaterials for integration with 3-D bioprinting." *Annals of biomedical engineering* 43.3 (2015): 730-746.
28. Wüst, Silke, et al. "Tunable hydrogel composite with two-step processing in combination with innovative hardware upgrade for cell-based three-dimensional bioprinting." *Acta biomaterialia* 10.2 (2014): 630-640.
29. Parisi-Amon, Andreina et al. "Protein-engineered injectable hydrogel to improve retention of transplanted adipose-derived stem cells." *Advanced healthcare materials* vol. 2,3 (2013): 428-32. doi:10.1002/adhm.201200293
30. Gopinathan, Janarthanan, and Insup Noh. "Recent trends in bioinks for 3D printing." *Biomaterials research* vol. 22 11. 6 Apr. 2018, doi:10.1186/s40824-018-0122-1
31. Colosi, Cristina et al. "Microfluidic Bioprinting of Heterogeneous 3D Tissue Constructs Using Low-Viscosity Bioink." *Advanced materials (Deerfield Beach, Fla.)* vol. 28,4 (2016): 677-84. doi:10.1002/adma.201503310
32. Yin, Jun, et al. "3D bioprinting of low-concentration cell-laden gelatin methacrylate (GelMA) bioinks with a two-step cross-linking strategy." *ACS applied materials & interfaces* 10.8 (2018): 6849-6857.
33. Junttila, Melissa R., and Frederic J. de Sauvage. "Influence of tumour micro-environment heterogeneity on therapeutic response." *Nature* 501.7467 (2013): 346-354.
34. Ishii, Genichiro, Atsushi Ochiai, and Shinya Neri. "Phenotypic and functional heterogeneity of cancer-associated fibroblast within the tumor microenvironment." *Advanced drug delivery reviews* 99 (2016): 186-196.
35. Riching, Kristin M et al. "3D collagen alignment limits protrusions to enhance breast cancer cell persistence." *Biophysical journal* vol. 107,11 (2014): 2546-58. doi:10.1016/j.bpj.2014.10.035
36. Seano, Giorgio, et al. "Modeling human tumor angiogenesis in a three-dimensional culture system." *Blood, The Journal of the American Society of Hematology* 121.21 (2013): e129-e137.

37. Midha, Swati, et al. "Advances in three-dimensional bioprinting of bone: Progress and challenges." *Journal of tissue engineering and regenerative medicine* 13.6 (2019): 925-945.
38. Jiang, Tao, et al. "Bioprintable Alginate/Gelatin Hydrogel 3D In Vitro Model Systems Induce Cell Spheroid Formation." *JoVE (Journal of Visualized Experiments)* 137 (2018): e57826.
39. McBeth, Christine, et al. "3D bioprinting of GelMA scaffolds triggers mineral deposition by primary human osteoblasts." *Biofabrication* 9.1 (2017): 015009.
40. Fairbanks, Benjamin D et al. "Photoinitiated polymerization of PEG-diacrylate with lithium phenyl-2,4,6-trimethylbenzoylphosphinate: polymerization rate and cytocompatibility." *Biomaterials* vol. 30,35 (2009): 6702-7.
doi:10.1016/j.biomaterials.2009.08.055
41. Pati, Falguni, et al. "Printing three-dimensional tissue analogues with decellularized extracellular matrix bioink." *Nature communications* 5.1 (2014): 1-11.